Eur. Phys. J. Appl. Phys. **34**, 7–12 (2006)
DOI: 10.1051/epjap:2006039

THE EUROPEAN PHYSICAL JOURNAL APPLIED PHYSICS

Transparent conducting ZnO-CdO thin films deposited by e-beam evaporation technique

H.A. Mohamed[a], H.M. Ali, S.H. Mohamed, and M.M. Abd El-Raheem

Physics Department, Faculty of Science, South Valley University, 82524 Sohag, Egypt

Received: 29 November 2005 / Received in final form: 21 February 2006 / Accepted: 24 February 2006
Published online: 4 May 2006 –

Abstract. Thin films of Zn_{1-x} Cd_xO with $x = 0$, 0.1, 0.2, 0.3, 0.4 and 0.5 at.% were deposited by electron-beam evaporation technique. It has been found that, for as-deposited films, both the transmittance and electrical resistivity decreased with increasing the Cd content. To improve the optical and electrical properties of these films, the effect of annealing temperature and time were taken into consideration for Zn_{1-x} Cd_xO film with $x = 0.2$. It was found that, the optical transmittance and the electrical conductivity were improved significantly with increasing the time of annealing. At fixed temperature of 300 °C, the transmittance increased with increasing the time of annealing and reached its maximum values of 81% in the visible region and 94% in the NIR region at annealing time of 120 min. The low electrical resistivity of 3.6×10^{-3} Ω cm was achieved at the same conditions. Other parameters named free carrier concentrations, refractive index, extinction coefficient, plasma frequency, and relaxation time were studied as a function of annealing temperature and time for 20% Cd content.

PACS. 61.10.-i X-ray diffraction and scattering – 78.66.-w Optical properties of specific thin films – 73.61.-r Electrical properties of specific thin films – 73.50.-h Electronic transport phenomena in thin films

1 Introduction

Transparent conducting oxides (TCOs) are a class of materials that transmit visible radiation and conduct electricity. They find application as transparent electrodes in numerous applications such as photovoltaics, flat panel displays, heat reflective coatings on energy-efficient windows, and electrochromics such as smart mirrors [1–3]. Zinc oxide (ZnO) holds considerable interest as an optical transparent material due to its wide band gap (3.3 eV), its amenability to defects or impurity doping and other desirable properties such as low cost and non-toxicity [4], while pure ZnO films present high values of resistivity [5]. CdO is an n type semiconductor, with a well-established direct band gap at approximately (2.4–2.7 eV) and a poor optical transmittance in the visible spectral region [6]. When compared with ZnO, the transmittance of CdO in the visible region of the spectrum has been reported as rather low. However, cadmium oxide is characterized by a much lower resistivity [6]. Hence, it could directly combine the optical and electrical properties of an alloy of cadmium and zinc oxides, making it useful for its application in solar cells.

A variety of methods have been reported for the preparation of ZnO and CdO thin films like sol-gel [6], spray pyrolysis [5,7–10], laser ablation [11] and thermal evaporation [12]. On the other hand, as for as we know, $Zn_{1-x}Cd_xO$ has not yet been previously studied by e-beam evaporation technique.

In this work, undoped and CdO doped ZnO thin films have been deposited by electron beam evaporation technique. The effect of compositions and annealing temperature on the structural, optical, and electrical properties of these films were investigated.

2 Experimental techniques

Portions of powdered highly pure (99.999%) of ZnO and CdO were grinded separately by means of an agate mortar and pestle. Mixture of $(ZnO)_{1-x}$: $(CdO)_x$ has been prepared using suitable ratios of ($x = 0$, 0.1, 0.2, 0.3, 0.4 and 0.5). To insure complete mixing, these mixtures have been grinded together for at least three hours. Then they have been made in tablets form using a cold pressing technique. In order to increase the diffusion process and consequently improve the homogeneity of the material, the prepared tablets were heated at 850 °C for 4 h in air.

Thin films of the prepared Zn_{1-x} Cd_xO ($x = 0$, 0.1, 0.2, 0.3, 0.4 and 0.5) tablets were deposited onto ultrasonically cleaned glass substrates using Edwards high vacuum coating unit model E306A. The evaporation conditions were: (1) a vacuum of 2×10^{-5} torr, (2) an accelerating voltage of 3 kV, (3) electron beam current 8–14 mA, and (4) the substrate temperature of 60 °C. The rate of evaporation was controlled within the range

[a] e-mail: hus49@hotmail.com

10–15 nm/min. The film thickness (∼200 nm) and deposition rate were controlled by means of a digital film thickness monitor model TM200 Maxtek. Investigations of the microstructure was carried out on Phillips (PW-1710) Cu-K_α diffractometer XRD ($\lambda = 1.541838$ Å) by varying diffraction angle 2θ from 4 to 70 by step width of 0.04 in order to evaluate crystalline phase and crystallite orientation.

A Jasco model V-570 (UV-Visible-NIR) double beam Spectrophotometer (with photometric accuracy of ± 0.002–0.004 Abs. and $\pm 0.3\%$ Trans.) was employed to record the transmission T and reflection R spectra over the wavelength range from 200 to 2500 nm at normal incidence. The absorption coefficient α of the films was determined directly from the spectrophotometer readings using the formula [13]:

$$\alpha = \frac{2.303}{d} \log_{10}\left(\frac{1-R}{T}\right) \tag{1}$$

where d is the film thickness, T is the transmittance and R is the reflection of the film.

The optical energy band gap was estimated from the optical measurements by analyzing the optical data with the expression for the optical absorbance, and the photon energy, $h\nu$ using the following equation:

$$(\alpha h\nu)^2 = A(h\nu - E_g) \tag{2}$$

where α represents the absorption coefficient, h is the Planck's constant, A is a constant and E_g is the optical energy band gap, which were obtained by extrapolating the linear portion of the plots of $(ahv)^2$ versus $h\nu$ to $\alpha = 0$.

The refractive index n was calculated from the following equation:

$$n = \frac{1+R}{1-R} \pm \left[\left(\frac{R+1}{R-1}\right)^2 - \left(1+k^2\right)\right]^{1/2} \tag{3}$$

where $k = \alpha\lambda/4\pi$ is the extinction coefficient and λ is the incident light wavelength. In the present work, more reasonable values for n may be determined by considering the plus sign of equation (3).

Using Drude's theory of dielectrics, the real part (ε_1) of the complex dielectric function ε can be written as [14]

$$\varepsilon_1 = n^2 - k^2 = \varepsilon_\infty - \frac{e^2}{\pi c^2}\frac{N}{m^*}\lambda^2 \tag{4}$$

where ε_∞ is the residual dielectric constant, c is the light velocity, N is the free carrier concentration, m^* is the electron effective mass, which was chosen based on the observed data of other workers ($m^* = 0.24\, m_o$ for either ZnO or CdO) [15,16], e is the electronic charge (1.6×10^{-19} C). By plotting ε_1 versus λ^2, the values of slope and intercept yield the free carrier concentration and the residual dielectric constant ε_∞. On the other hand, the plasma frequency which for one kind of free carriers is given by

$$\omega_p = \left(\frac{Ne^2}{\varepsilon_o \varepsilon_\infty m^*}\right)^{1/2} \tag{5}$$

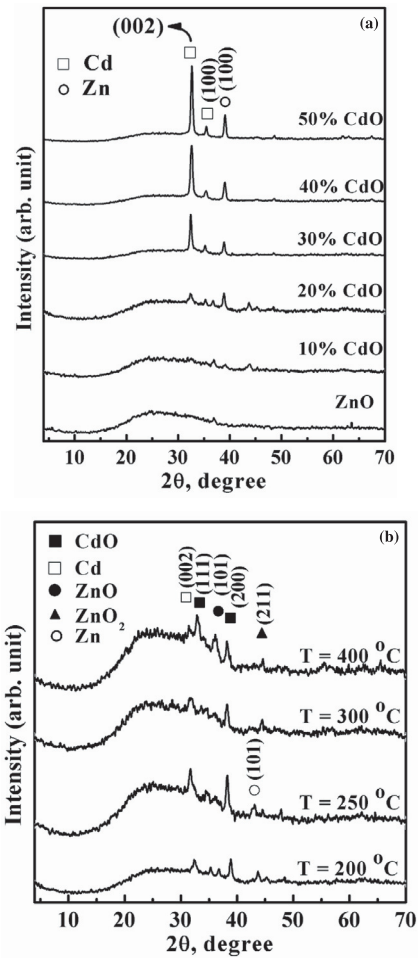

Fig. 1. X-ray diffraction of as-deposited Zn_{1-x} Cd_xO thin films as a function of Cd content (a) and as a function of annealing temperature (b).

where ε_o is the permittivity of free space.

The relaxation time, τ, has been obtained using the imaginary part (ε_2) of the complex dielectric function by plotting ε_2 versus λ^3 in the following equation:

$$\varepsilon_2 = 2nk = \frac{\varepsilon_\infty \omega_p^2}{4\pi^3 c^3 \tau}\lambda^3. \tag{6}$$

The film resistivity measurements were carried out at room temperature using a Keithley 614 electrometer with simple two-probe contacts. Silver paste electrodes with separation of 2 mm were used.

3 Results and discussions

Figure 1a shows the X-ray diffraction patterns of as-deposited Zn_{1-x} Cd_xO films. It is seen that ZnO film exhibits an amorphous structure. The addition of CdO content leads to crystalline peaks. From the JCDPS cards, the diffraction peaks can be identified as unoxidized Cd and Zn. It is clear also that, films have three prominent peaks

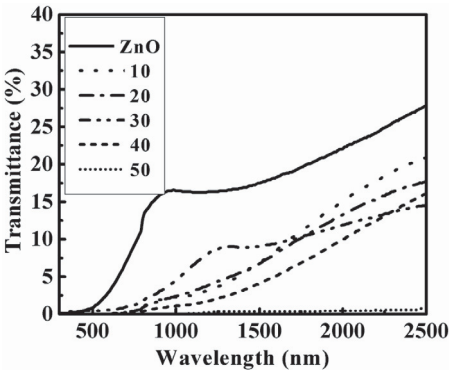

Fig. 2. The spectra of transmittance of as-deposited Zn_{1-x} Cd_xO thin films in the wavelength range from 200 to 2500 nm for different Cd content.

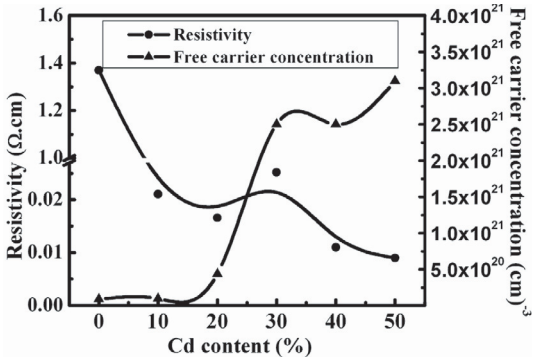

Fig. 3. Variation of the electrical resistivity and carrier concentration for as-deposited Zn_{1-x} Cd_xO thin films at room temperature.

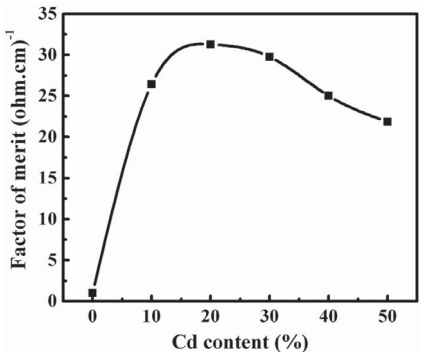

Fig. 4. Variation of the factor of merit φ for as-deposited Zn_{1-x} Cd_xO thin films with Cd content.

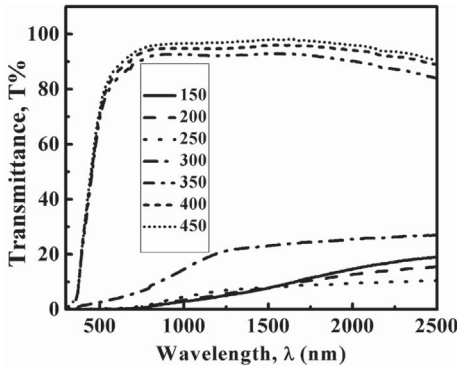

Fig. 5. Spectral variation of the transmittance $T\%$ with wavelength (nm) for Zn_{1-x} Cd_xO thin films with $x = 0.2$ at different annealing temperatures.

of (100), (002), and (100) for Cd and Zn respectively, indicating that the structure has been changed from amorphous to polycrystalline. The intensities of these peaks were found to be enhanced with increasing the concentration of Cd content.

The effect of annealing temperature on the structural properties of Zn_{1-x} Cd_xO film with $x = 0.2$ is shown in Figure 1b. The diffraction patterns indicate that, the films are polycrystalline in nature with cubic structure. It has been found that, with increasing the annealing temperature from 200 to 400 °C cadmium and zinc elements started to oxidize. The diffraction peaks (200), (111) corresponding to CdO and (101) ZnO could be observed for annealed films and seem to increase in intensities with increasing the temperature of annealing due to the improvement in the crystallinity of the films. In addition, it is noticed that, the intensity of Cd (002) and Zn (101) peaks increases with increasing the annealing temperature up to 250 °C. With further increase of annealing temperature, Zn (101) peak disappear and Cd (002) peak gradually decreased. Figure 2 shows the wavelength dependence of optical transmittance of as-deposited Zn_{1-x} Cd_xO films. It is evident that, all films exhibit poor optical transmittance because of the film opaqueness. This opaqueness is due to the appearance of Zn and Cd elements which refers to the large number of oxygen deficiency as shown in Figure 1a. It is evident also that the transmittance decreases with increasing Cd content. On the other hand, it is clear from Figure 3 that, the calculated values of the free carrier concentrations belonging to these films seen to have high values. These carriers contribute to decrease the film resistivity and at the same time contribute to increase the free carriers absorption, which lead to decrease the transmittance [17,18]. Figure 3 also shows the electrical resistivity measured at room temperature as a function of Cd content for as-deposited films. It is obvious that, the electrical resistivity decreases with increasing the Cd content, which can be attributed to the enhancement of the film crystallinity because of degenerate property of CdO and due to the increase of the free carrier concentrations. The behavior of carrier concentration is in good agreement with Drude's theory, since the charge carrier concentration is directly related to the conductivity of the material [19,20].

The quality of a transparent conducting oxide will be judged by the parameter of factor of merit, $\varphi = T_m/\rho$ [21] where T_m is the average transmittance in the visible region and ρ is the electrical resistivity. As shown in Figure 4 the factor of merit φ, has a maximum value for Zn_{1-x} Cd_xO with $x = 0.2$. So the effect of heat treatment is taken under consideration only for $x = 0.2$.

The effect of annealing temperature in the range from 200 to 450 °C on the optical transmittance of Zn_{1-x} Cd_xO film with $x = 0.2$ is shown in Figure 5. It is clear that, with

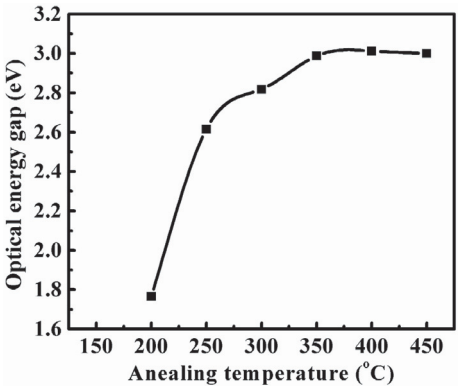

Fig. 6. Variation of the optical band gap E_g with annealing temperature for 15 min.

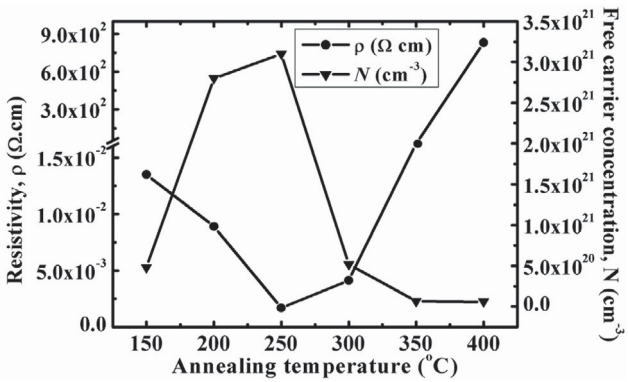

Fig. 7. Plot of the electrical resistivity ρ and the free carrier concentration for Zn_{1-x} Cd_xO films with $x = 0.2$ annealed at different temperatures for 15 min.

increasing the annealing temperature, the transmittance increases and reaches 86% (at absorption edge) and about 98% in NIR region at temperature of annealing 350 °C. As the temperature of annealing increases over 350 °C, there is no significant increase in transmittance. It means that the oxygen vacancies reduced greatly after annealing in air.

The direct optical energy gap as a function of annealing temperature is plotted in Figure 6. It is clear that, the optical energy band gap increases with increasing the annealing temperature. The increase in the band gap energy with increasing the temperature of annealing up to 250 °C can be attributed to the Burstein-Moss shift in which the absorption edge shifts towards higher energy with an increase of carrier concentration [22,23]. The slightly increase in the optical energy gap at temperature of annealing over than 250 °C, may be due to that, the unsaturated defects are gradually annealed out producing a larger number of saturated bonds; this decreases the density of localized states and consequently the optical gap increased [21,24]. It means that oxygen vacancies gradually decreased after annealing in air. Figures 1b, 5 and 7 confirm the situation. It is also observable that the highest value of energy gap is about 3.01 eV at annealing temperature of 400 °C.

Figure 7 shows the variations of both the resistivity (ρ) and the free carrier concentration (N) for Zn_{1-x} Cd_xO film ($x = 0.2$) with annealing temperature for 15 min. It is seen that the electrical resistivity decreases with increasing the temperature of annealing, reaching its minimum value of 1.68×10^{-3} Ω cm at annealing temperature 250 °C. At higher value of annealing temperature, the measured resistivity increases with increasing the temperature of annealing. The decrease in the electrical resistivity is considered to be caused by the desorption of oxygen from the Zn_{1-x} Cd_xO film surface. When the films are annealed under ambient air at temperature higher than 250 °C, oxygen is chemisorbed on the film surface and in pores, acting as an acceptor by accepting an electron from occupied conduction band states, resulting in very high surface resistivity [6]. Furthermore, the adsorbed oxygen removes zinc interstitials and/or oxygen vacancies, thus reduce the density of donors like defects and carrier concentration [25]. Therefore, the obtained behavior of electrical resistivity is in good agreement with some previous works [6,9,26,27].

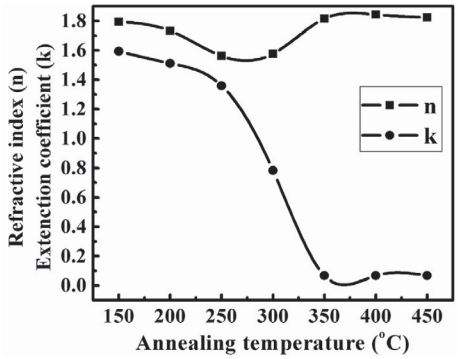

Fig. 8. Variations of the refractive index (n) and extinction coefficient (k) in the visible region with annealing temperature.

Figure 8 depicts the variation of the refractive index (n) and extinction coefficient (k) calculated at wavelength 550 nm as a function of annealing temperature. It is seen that, the refractive index decreases from 1.79 to 1.56 with increasing the temperature of annealing up to 250 °C and then starts to increase, reaching the value of 1.82 at annealing temperature of 450 °C. On the other hand, the extinction coefficient (k) decreases with increasing the annealing temperature, which can be attributed to the increase of the film transparency.

As described in the experimental section, that the optical parameters namely plasma frequency and relaxation time were calculated using equations (5, 6). The dependence of these two parameters on the annealing temperature is shown in Figure 9. It is noticed that, the plasma frequency increases up to annealing temperature of 250 °C and then starts to decrease with increasing the temperature of annealing. It is seen also from Figures 7 and 9 that, the plasma frequency is directly proportion with the free carrier concentration. This result is in good agreement with Drude's theory. On the other hand, it is known that, the relaxation time is inversely proportion with the free carrier concentration and

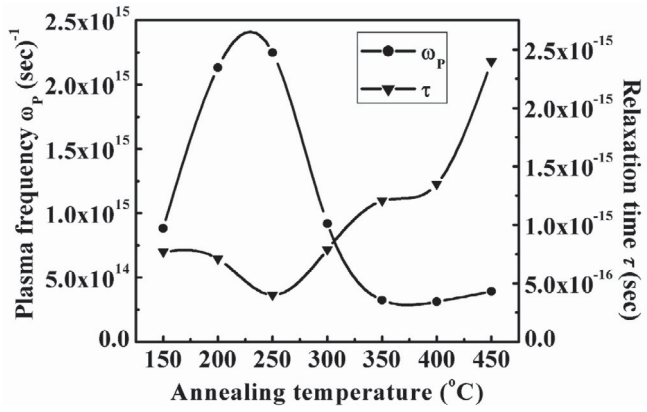

Fig. 9. Variation of the plasma frequency and relaxation time as a function of annealing temperature.

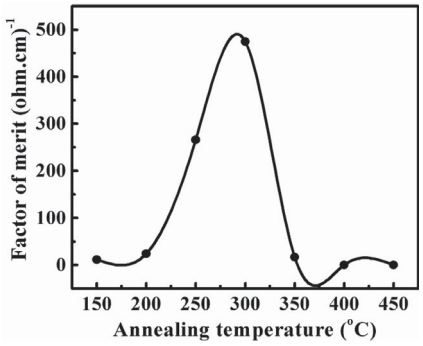

Fig. 10. Annealing temperature dependence of the factor of merit φ for Zn_{1-x} Cd_xO film with $x = 0.2$.

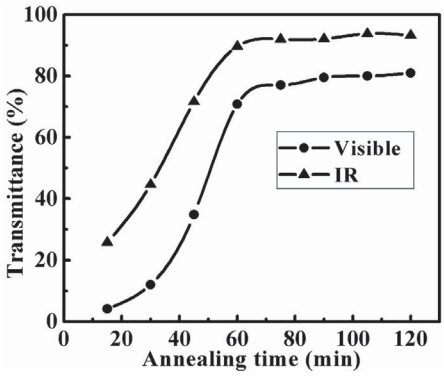

Fig. 11. The average transmittance in the visible and near infrared regions as a function of annealing time at 300 °C.

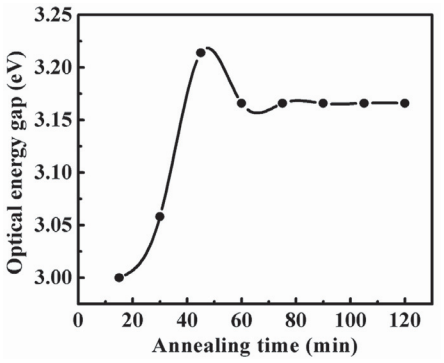

Fig. 12. Variation of the optical band gap as a function of annealing time at 300 °C.

therefore, it has an opposite behavior of the free carrier concentration.

In order to predict the selective properties of transparent conductive coatings from the fundamental optical and electrical properties, the factor of merit can be employed. Figure 10 shows the variation of the factor of merit as a function of annealing temperature. The figure indicates that the best value of annealing temperature is at 300 °C. So the effect of annealing time on the optical and electrical properties of the prepared film with $x = 0.20$ will taken into account at this value of temperature.

As shown in Figure 11, with increasing the annealing time (15–120 min) the transmittance increases to reach 81% in the visible region and about 94% in NIR region at annealing temperature of 300 °C for 120 min. In addition, the direct optical energy gap increases with increasing the time of annealing to reach 3.21 eV at 45 min. No significant variation is observed in the energy gap for further increasing in the time of annealing as seen in Figure 12.

The electrical resistivity and the calculated optical mobility as a function of annealing time are shown in Figure 13a. It is noticed that, the resistivity decreases with prolongation the annealing times up to 60 min, and saturates for longer times. This may be due to the decrease of the grain-boundary scattering and the grain size growth. Therefore, the resistivity reduction can be explained as very likely due to the increase of the electron mobility as a consequence of the crystallite size growth with annealing times. Figure 13b presents the change of the free carrier concentration of Zn_{1-x} Cd_xO film of $x = 0.2$ with annealing time at 300 °C. It is quiet clear that the carrier concentration decreases with increasing the time of annealing; this may be due to the reduction of the oxygen vacancy in the film after annealing in air.

The reflective index (n), extinction coefficient (k) and plasma frequency (ω_P) are listed in Table 1. It is found that the refractive index is inversely related to the carrier concentration.

4 Conclusion

Thin films of Zn_{1-x} Cd_xO with $x = 0$, 0.1, 0.2, 0.3, 0.4 and 0.5, have been deposited by electron beam evaporation technique. The effect of cadmium content and heat treatment on the electrical, optical and structural properties of these films was carried out. For as-deposited films, it has been found that, the transmittance, and resistivity were decreased with increasing the Cd content. Moreover, for 20% Cd content it is found that, the transmittance increased with increasing the temperature of annealing and attained its maximum value of 86% (at absorption edge) and about 98% in NIR region at 400 °C whereas, the electrical resistivity has found to be equal 8.3×10^2 Ω cm. The lowest resistivity of 1.68×10^{-3} Ω cm was obtained

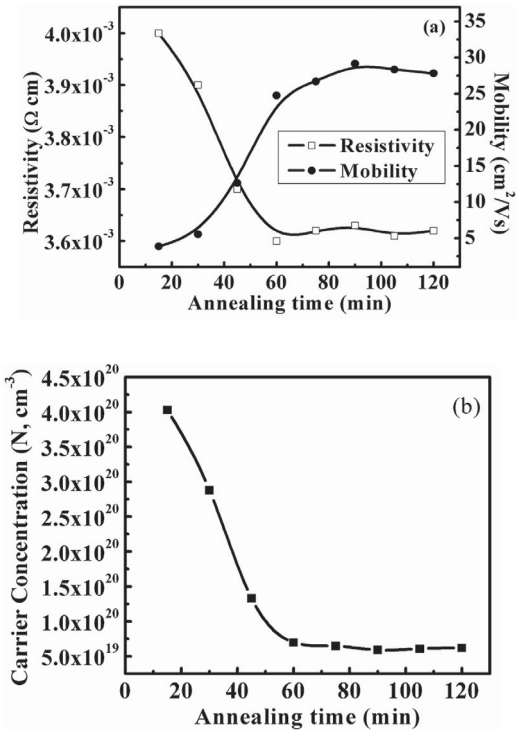

Fig. 13. Plot of (a) the annealing time dependent of electrical resistivity and the mobility carriers; and (b) the free carrier concentration for Zn_{1-x} Cd_xO films with $x = 0.2$.

Table 1. Variation of the refractive index (n), extinction coefficient k and plasma frequency ω_P with different annealing time at 300 °C.

Annealing time [min]	n [$\lambda = 550$ nm]	k [$\lambda = 550$ nm]	ω_P [10^{14} s^{-1}]
15	1.44	0.727	8.109
30	1.45	0.497	6.849
45	1.50	0.265	2.319
60	1.67	0.111	3.070
75	1.71	0.092	3.242
90	1.71	0.085	2.910
105	1.78	0.084	3.639
120	1.79	0.081	3.668

at annealing temperature of 250 °C while, the average transmittance is not exceed 8% either in the visible or NIR regions. At fixed temperature of 300 °C, the transmittance increased with increasing the time of annealing to reach its maximum values of 81% in the visible region and 94% in the NIR region at annealing time of 120 min. The Optical band gap is found to be equal 3.17 eV. The electrical resistivity of 3.6×10^{-3} Ω cm was obtained at the same conditions. These results confirm that Zn_{1-x} Cd_xO with $x = 0.2$, annealed at 300 °C for 120 min is useful for various optoelectronic applications as a transparent conducting oxide. Using Drude's model, the free carrier concentrations, refractive index, extinction coefficient, plasma frequency, and relaxation time were studied as a function of annealing temperature and time for 20% Cd content. It has been found that these parameters were in good agreement with the Drude's model.

The authors would like to thank Prof. Dr. E.Kh. Shokr and Prof. Dr. M.M. Wakkad for their continuous encouragement and comments.

References

1. R. Jayakrishnan, G. Hodes, Thin Solid Films **440**, 19 (2003)
2. P.K. Biswasa, A. Dea, N.C. Pramanika, P.K. Chakraborty, K. Ortner, V. Hock, S. Korder, Mater. Lett. **57**, 2326 (2003)
3. S. Yamammoto, T. Yamanaka, Z. Ueda, J. Vac. Sci. Technol. A **5**, 1952 (1987)
4. P. Sagar, M. Kumar, R.M. Mehra, Thin Solid Films **489**, 94 (2005)
5. O. Vigil, F. Cruz, G. Santana, L. Vailllant, A. Morales-Acevedo, G. Contreras-Puente, Appl. Surf. Sci. **161**, 27 (2000)
6. Y.S. Choi, C.G. Lee, S.M. Cho, Thin Solid Films **298**, 153 (1996)
7. G. Santana, A. Morales-Acevedo, O. Vigil, F. Cruz, G. Contreras-Puente, L. Vaillant, Superficies Vacio **9**, 300 (1999)
8. H. Tabet-Derraz, N. Benramdance, D. Nacer, A. Bouzidi, M. Medles, Sol. Energ. Mat. Sol. C **73**, 249 (2002)
9. H.T. Derraz, N. Benramdance, D. Nacer, A. Bouzidi, M. Medles, Sol. Energ. Mat. Sol. C **73**, 249 (2002)
10. F.C. Gandarilla, A.M. Acevedo, O. Vigil, M.H. Garduno, L. Vaillant, G.C. Puente, Mater. Chem. Phys. **78**, 840 (2003)
11. C. Messaoudi, D. Sayah, Abd-Lefdil, Phys. Status Solidi A **151**, 93 (1995)
12. M. Dinesau, P. Verardi, Appl. Surf. Sci. **106**, 149 (1996)
13. H.M. Ali, Phys. Status Solidi A **202**, 2742 (2005)
14. T.S. Moss, G.J. Burrell, B. Ellis, *Semiconductor Optoelectronics* (Butterworths, London, 1973)
15. V.A. Fonoberov, A.A. Balandin, Appl. Phys. Lett. **85**, 5971 (2004)
16. R. Asahi, A. Wang, J.R. Babcock, N.L. Edleman, A.W. Metz, M.A. Lane, V.P. Dravid, C.R. Kannewurf, A.J. Freeman, T.J. Marks, Thin Solid Films **411**, 101 (2002)
17. C.G. Granqvist, A. Hultaker, Thin Solid Films **411**, 1 (2002)
18. X. Wu, T.J. Coutts, W.P. Mulligan, J. Vac. Sci. Technol. A **15**, 1057 (1997)
19. F. Wooten, *Optical Properties of Solids* (Academic Press, San Diego, 1972)
20. S.H. Brewer, S. Franzen, Chem. Phys. **300**, 285 (2004)
21. H.M. Ali, H.A. Mohamed, S.H. Mohamed, Eur. Phys. J. Appl. Phys. **31**, 87 (2005)
22. E. Burstein, Phys. Rev. **93**, 632 (1954)
23. T.S. Moss, Proc. Phys. Soc. London B **67**, 775 (1954)
24. E. Abd El-Wahabb, M.M. El-Samanoudy, M. Fadel, Appl. Surf. Sci. **174**, 106 (2001)
25. S.H. Mohamed, H.M. Ali, H.A. Mohamed, A.M. Salem, Eur. Phys. J. Appl. Phys. **31**, 95 (2005)
26. S.N. Qiu, C.X. Qiu, I. Shih, Sol. Energ. Mater. **16**, 471 (1987)
27. S.H. Mohamed, Phys. Status Solidi A **202**, 1948 (2005)